Effective Forces Between Quantum Bound States

Alexander Rokash,[1] Evgeny Epelbaum,[1,2] Hermann Krebs,[1,2] and Dean Lee[3,2]
[1]Institut für Theoretische Physik II, Ruhr-Universität Bochum, D-44870 Bochum, Germany
[2]Kavli Institute for Theoretical Physics, University of California, Santa Barbara, California 93106-4030, USA
[3]Department of Physics, North Carolina State University, Raleigh, North Carolina 27695, USA
(Received 13 January 2017; revised manuscript received 7 April 2017; published 9 June 2017)

Recent *ab initio* lattice studies have found that the interactions between alpha particles (^{4}He nuclei) are sensitive to seemingly minor details of the nucleon-nucleon force, such as interaction locality. In order to uncover the essential physics of this puzzling phenomenon without unnecessary complications, we study a simple model involving two-component fermions in one spatial dimension. We probe the interaction between two bound dimers for several different particle-particle interactions and measure an effective potential between the dimers using external point potentials which act as numerical tweezers. We find that the strength and range of the local part of the particle-particle interactions play a dominant role in shaping the interactions between the dimers and can even determine the overall sign of the effective potential.

DOI: 10.1103/PhysRevLett.118.232502

We investigate the connection between microscopic particle interactions and the cohesion responsible for the formation of complex structures such as nuclei. In atomic physics, the van der Waals force describes the interaction between neutral spherical atoms due to induced electric dipoles. The quantum mechanical description was first derived by London using second-order perturbation theory [1]. A similar phenomenon occurs between alpha particles or ^{4}He nuclei, with the two-pion exchange potential playing an important role [2,3]. However, the physics of this system is significantly more complicated due to the complexity of the nuclear forces and its delicate balance against Pauli repulsion between identical nucleons and the Coulomb interaction. In Ref. [3] a surprising result was found that the local or nearly local part of the nuclear interactions are important in determining the strength of the alpha-alpha interaction. In addition to being an interesting fundamental science question, understanding this phenomenon in more detail may lead to new avenues for improving the order-by-order convergence of *ab initio* nuclear structure calculations in medium mass nuclei [4–9] using chiral effective field theory. See Ref. [10] for a review of chiral effective field theory.

By a local force we mean that the positions of the particles are left in place during the interaction process, while the more general nonlocal force may change the relative separation between particles. We note that there is little difference between an exactly local interaction which keeps the particle positions exactly in place and a nearly local interaction which changes the particle positions only at length scales small compared to the quantum bound state size. Thus, when we use the term local we mean both cases. In this Letter we investigate whether this local dominance of the alpha-alpha interaction could be a general phenomenon. To head towards this goal, we start by examining the simplest possible quantum system in detail to help elucidate the general principles involved. For this task we study the residual interactions between two bound dimers in one spatial dimension. Before proceeding we should mention the pioneering work by Combescot and collaborators in understanding the interactions of composite bosons such as excitons composed of elementary fermions [11–15]. Our emphasis, though, is somewhat different as we focus on the impact of different particle-particle interactions upon the effective dimer-dimer interaction. In addition to the main nuclear physics motivation, the results of our lattice study should be useful in predicting the properties of composite bosons on optical lattices for different types of interactions, including single-site and nearest-neighbor interactions.

In our calculations we consider two-component fermions, which we label as up and down spins. As there are different conventions and units used in the nuclear, atomic, and condensed-matter communities, throughout our analysis we use only dimensionless lattice units. Our lattice Hamiltonian has the form

$$H = t\sum_{n,\sigma=\uparrow,\downarrow}[b_\sigma^\dagger(n+1)-b_\sigma^\dagger(n)][b_\sigma(n+1)-b_\sigma(n)] + \sum_{n,i,i'} b_\uparrow^\dagger\left(\frac{n+i}{2}\right) b_\downarrow^\dagger\left(\frac{n-i}{2}\right) I_{i,i'} b_\downarrow\left(\frac{n-i'}{2}\right) b_\uparrow\left(\frac{n+i'}{2}\right), \tag{1}$$

where n, i, i', $(n\pm i)/2$, and $(n\pm i')/2$ are restricted to have integer values. We take $t = 1/20$ in dimensionless lattice units. In nuclear physics notation, where t is usually written as $1/(2m)$, this corresponds with the dimensionless mass parameter $m = 10$. We consider five different interactions, and in the following we list all the nonzero terms. In all five cases the interaction produces a bound dimer

with dimensionless energy $-1/40$. The motivation for introducing the various versions of the two-particle interactions will be explained below. The first interaction is a pointlike interaction with

$$I^{(1)}_{0,0} = c^{(1)}, \tag{2}$$

where $c^{(1)} = -0.103078$. The second interaction is a local interaction that has a range of one lattice unit,

$$I^{(2)}_{0,0} = I^{(2)}_{1,1} = I^{(2)}_{-1,-1} = c^{(2)}, \tag{3}$$

with $c^{(2)} = -0.049851$. The third interaction is a local interaction that has a range of two lattice units,

$$I^{(3)}_{0,0} = I^{(3)}_{1,1} = I^{(3)}_{2,2} = I^{(3)}_{-2,-2} = I^{(3)}_{-1,-1} = c^{(3)}, \tag{4}$$

with $c^{(3)} = -0.038321$. The fourth interaction is a nonlocal interaction that has a range of two lattice units and only even-parity interactions,

$$I^{(4)}_{0,0} = c^{(4)}, \tag{5}$$

$$I^{(4)}_{1,1} = I^{(4)}_{2,2} = I^{(4)}_{-2,-2} = I^{(4)}_{-1,-1} = \frac{c^{(4)}}{2}, \tag{6}$$

$$I^{(4)}_{1,-1} = I^{(4)}_{2,-2} = I^{(4)}_{-2,2} = I^{(4)}_{-1,1} = \frac{c^{(4)}}{2}, \tag{7}$$

with $c^{(4)} = -0.038321$. The fifth interaction is another nonlocal interaction with range two lattice units and only even-parity interactions,

$$I^{(5)}_{0,0} = I^{(5)}_{2,2} = I^{(5)}_{-2,-2} = I^{(5)}_{-2,2} = I^{(5)}_{2,-2} = c^{(5)}, \tag{8}$$

$$I^{(5)}_{1,1} = I^{(5)}_{-1,-1} = I^{(5)}_{-1,1} = I^{(5)}_{1,-1} = \frac{c^{(5)}}{2}, \tag{9}$$

$$I^{(5)}_{0,2} = I^{(5)}_{2,0} = I^{(5)}_{-2,0} = I^{(5)}_{0,-2} = -c^{(5)}, \tag{10}$$

where $c^{(5)} = -0.052504$. In order to probe the effective forces between two dimers we apply an external potential of the form

$$U_{\rm ext}(n) = -u\sum_{n'} b^\dagger_\downarrow(n')b^\dagger_\downarrow(n+n')b_\downarrow(n+n')b_\downarrow(n'), \tag{11}$$

with coefficient $u > 0$. We refer to this external potential as numerical tweezers since for large-enough u the dimers will be held in place by the point potentials, with the localization length of the tweezer-bound dimer determining the spatial resolution of our external probe. This is illustrated in Fig. 1.

We have made the numerical tweezers translationally invariant by summing over n' in Eq. (11). This is convenient for the exact diagonalization calculations we do here. In other applications such as auxiliary-field Monte Carlo lattice simulations [3,16–19], a simpler tweezer potential with fixed ends is more convenient,

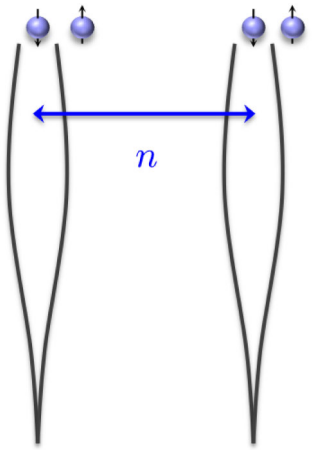

FIG. 1. Illustration of the external potential acting as numerical tweezers by holding the down-spin particles at separation distance n.

$$U_{\rm ext}(n) = -ub^\dagger_\downarrow(0)b^\dagger_\downarrow(n)b_\downarrow(n)b_\downarrow(0). \tag{12}$$

This numerical tweezer technique will be incorporated into future lattice simulations of nuclear structure.

We now compute the ground-state energy of the full Hamiltonian with external potential, $H + U_{\rm ext}(n)$, versus separation distance n. This energy, which we call the tweezer effective potential, is measured relative to its limiting value as $n \to \infty$. The tweezer effective potential measures the interaction energy between dimers as a function of separation distance. However, there is clearly also some dependence on the manner in which the tweezers are coupled to the dimers. The tweezers can be viewed as heavy particles which we have coupled to the down-spin particles. The tweezer effective potential is then the Born-Oppenheimer potential between the heavy particles induced by the dimer-dimer interaction.

In all the results presented here, we choose the tweezer coupling so that the tweezer binding energy is comparable to the dimer binding energy, and so the spatial resolution of our probe is comparable to the dimer size. Figure 2 shows

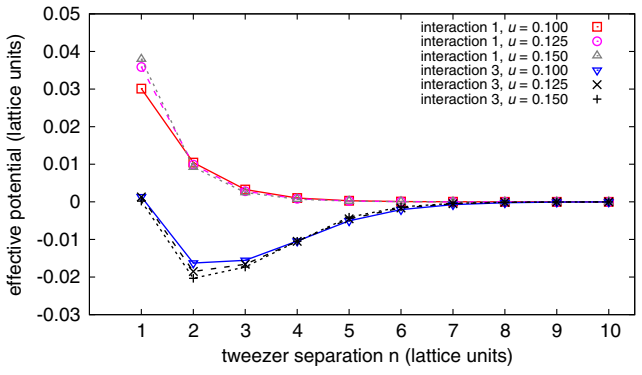

FIG. 2. The tweezer effective potential potential versus separation distance for interactions 1 and 3 for dimer binding energy $1/40$ and tweezer couplings $u = 0.100, 0.125, 0.150$.

the tweezer effective potential versus separation distance for interactions 1 and 3 and tweezer couplings $u = 0.100$, 0.125, 0.150. For $u = 0.100$ the tweezer binding energy is about half the dimer binding energy, while for $u = 0.150$ it is about the same as the dimer binding energy. We see that while there is some dependence on u, a fairly consistent shape can be seen for each interaction. What is striking is the large difference between the effective potentials. For interaction 1 it is purely repulsive while for interaction 3 it is attractive for every separation distance $n > 1$.

We now analyze the differences between the interactions more systematically. Figure 3 shows the tweezer effective potential versus separation distance for tweezer coupling $u = 0.100$ and interactions 1–5. As noted above, the dimer binding energy for all five interactions has the same value, $1/40$. In all cases we observe that the effective potential becomes more repulsive at short distances, with about the same slope between points $n = 1$ and $n = 2$ in all five cases. This suggests that the physics of Pauli repulsion is dominant at short distances. We note that the tweezer effective potential is not well defined for $n = 0$ due to the Pauli exclusion principle.

Let us now compare interactions 1, 2, and 3. Each of the interactions 1,2, and 3 are local step potentials with radii equal to 0,1, and 2 lattice units, respectively. We observe that the attraction between dimers increases with the range of the local interaction. As the range increases, the particles are able to interact from longer distances. This makes it easier for opposite-spin particles to attract each other while avoiding the strong Pauli repulsion between identical fermions. We note also that by increasing the range of the local interaction, the attraction in the odd-parity channel increases.

We now compare the tweezer effective potentials for interactions 3 and 4. The attraction between the dimers is rather strong for interaction 3 while interaction 4 is mostly repulsive. By design we have made interactions 3 and 4 identical in the even-parity channel, and so the dimer wave functions are exactly the same. However, interaction 4 contains a nonlocal exchange potential that removes all of the interaction strength in the odd-parity channel. Therefore, one can view the difference between the effective potentials for interactions 3 and 4 as arising from attractive odd-parity interactions in interaction 3 that are completely missing from interaction 4. This is an appealing and simple explanation. We can view the dimers as closed-shell bound states for the even-parity or "S-wave" interactions, and the attraction between dimers is due to odd-parity or "P-wave" interactions between closed-shell dimers.

However, this is not the full story. To illustrate we now turn our attention to the effective potential for interaction 5. Interaction 5 is like interaction 4 in that the nonlocal exchange potential removes all the odd-parity interactions. However, the effective potential is even more attractive for interaction 5 than for interaction 3. How can this be?

An answer to this puzzle emerges when we plot the local part of the particle-particle interaction $I_{i,i}$ versus relative particle separation i. This is shown in Fig. 4. We see that the local part of interaction 4 is weaker than that of interaction 3, while the local part of interaction 5 is stronger. This finding is entirely consistent with the conclusions of Ref. [3]. The strength of the local part of the interaction appears to play a dominant role in the effective forces between quantum bound states.

Our earlier explanation of the difference between interactions 3 and 4 being due to attractive odd-parity interactions can be rolled neatly into this notion of local dominance. We see in Fig. 4 that the odd-parity interactions contained in interaction 3 are responsible for enhancing the strength of the local part of the interaction relative to interaction 4. Thus, one can say that the difference between interactions 3 and 4 is either due to the attractive odd-parity interactions or due to the strength of the local interactions. Both explanations are equivalent.

The connection between local dominance and attractive higher-partial waves will persist in higher dimensions as well. In order to show this we make a brief detour and

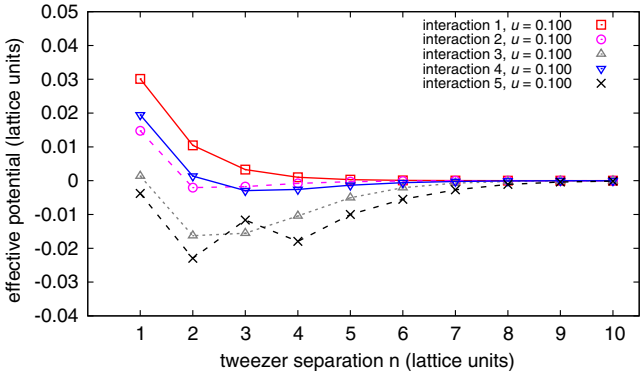

FIG. 3. The tweezer effective potential versus separation distance for interactions 1–5 for dimer binding energy $1/40$ and tweezer coupling $u = 0.100$.

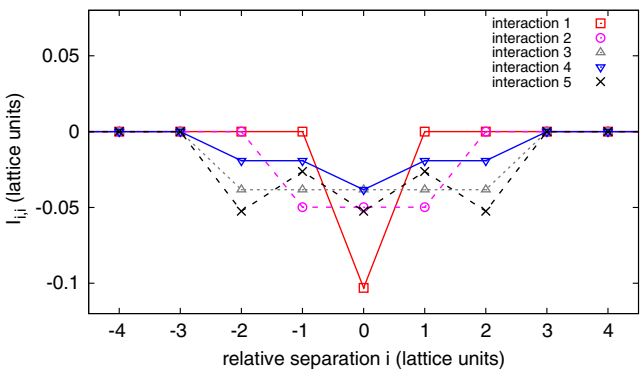

FIG. 4. Local part of the particle-particle interaction $I_{i,i}$ versus relative particle separation i for interactions 1–5 and dimer binding energy $1/40$.

consider a continuum S-wave two-body interaction in three dimensions. The explicit projection onto the S-wave produces nonlocality with respect to the incoming and outgoing angles. The angular integral kernel of the S-wave projection operator has the form

$$Y^*_{0,0}(\theta,\phi)Y_{0,0}(\theta',\phi'), \tag{13}$$

where Y_{L,L_z} denote spherical harmonics, (θ',ϕ') are the orientation angles of the incoming relative separation vector between the particles, $\mathbf{r}' = \mathbf{r}_2{}' - \mathbf{r}_1{}'$, and (θ,ϕ) are the orientation angles of the outgoing relative separation vector between the particles, $\mathbf{r} = \mathbf{r}_2 - \mathbf{r}_1$. When the interaction is sufficiently attractive, an S-wave bound state will form.

We now include an additional attractive interaction in partial wave L. For $L > 0$ and without partial wave mixing, this will have no impact on the S-wave bound-state wave function or binding energy. The angular integral kernel of the projection operator onto partial wave L has the form

$$\sum_{L_z} Y^*_{L,L_z}(\theta,\phi)Y_{L,L_z}(\theta',\phi'). \tag{14}$$

We note that the closure relation,

$$\sum_{L_z} Y^*_{L,L_z}(\theta,\phi)Y_{L,L_z}(\theta,\phi) = \frac{2L+1}{4\pi}, \tag{15}$$

implies that any attractive interaction in partial wave L will increase the attraction in the part of the interaction that is local with respect to angular orientation, $(\theta,\phi) = (\theta',\phi')$. This shows the direct connection between local dominance and attractive higher-partial waves. We mention that our arguments above are related to the well-known result that if a local potential is attractive at every point, it will be attractive in all partial waves.

We now return back to the one-dimensional system at hand. A closer look at the tweezer effective potential for interaction 5 shows unusual energy minima at separation distances $n = 2$ and $n = 4$. To understand how this arises, we note that the local part of the interaction $I_{i,i}$ has a zigzag shape with energy minima at $i = 0$ and $i = \pm 2$. The locations of these energy minima overlap when the tweezer separations are at $n = 2$ or $n = 4$, thus creating deep minima where the up-spin particles can simultaneously feel the attractive potential due to both down-spin particles. The nonlinear response of the up-spin particles to this coherent alignment of the local minima in $I_{i,i}$ gives rise to the energy minima in the effective potential at $n = 2$ and $n = 4$.

By studying a simple system of interacting dimers in one spatial dimension we have discovered a rich phenomenology of dimer-dimer interactions and their connection to the underlying particle-particle interactions. In some cases, like interaction 1, we find that the interaction is purely repulsive. We note that this repulsive interaction between dimers for pointlike interactions carries over to the dimer-dimer interaction in three dimensions as well [20–22]. For other cases such as interaction 3 and interaction 5, we get a strongly attractive interaction between dimers. The strength and range of the local part of the interaction play a dominant role in determining the effective potential.

The reason why local interactions are important was already discussed in Ref. [3] in the context of the tight-binding approximation. In the tight-binding limit, where the bound state is a tightly bound compact object, local interactions keep the interacting particles in their original place and, therefore, add coherently. We note that the tight-binding limit with local interactions can be viewed as a classical limit where the bound-state wave function sits at the bottom of the potential energy surface. In contrast, a general nonlocal interaction will attempt to move particles into locations not interior to the compact bound states. In short, the local or nearly local interactions are dominant because they preserve spatial coherence.

We have seen that decreasing the range of the interaction with the dimer binding energy fixed makes the effective potential more repulsive. Our zero-range interaction 1 can be viewed as an example of the universal limit when the range of the interaction is much smaller than the dimer size. We can also see this universal behavior by decreasing the binding energy of the dimers. In Fig. 5 we show the tweezer effective potential versus separation distance for interactions 1–5 with dimer binding energy $1/100$ and tweezer coupling $u = 0.100$. The corresponding values of the couplings are $c_1 = -0.064031$, $c_2 = -0.027454$, $c_3 = -0.019684$, $c_4 = -0.019684$, and $c_5 = -0.031440$. We observe that overall the effective potential is less attractive, exhibiting universal behavior when the range of the interaction is much smaller than the dimer size.

Nevertheless, our analysis of the differences among the five cases is still valid. When we compare interactions 1, 2,

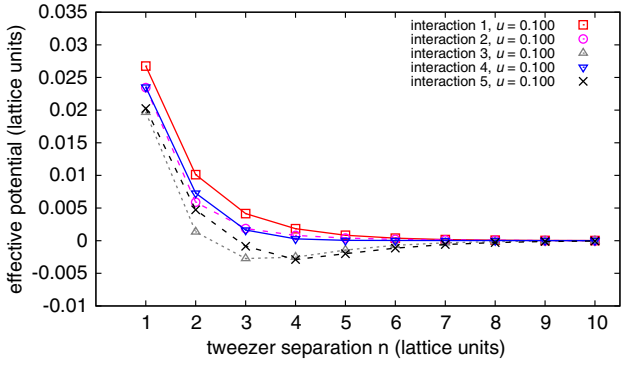

FIG. 5. The tweezer effective potential versus separation distance for interactions 1–5, with dimer binding energy $1/100$ and tweezer coupling $u = 0.100$.

and 3, the effective potential becomes more attractive as the range of the interaction is increased. The purely even-parity interaction 4 is less attractive than interaction 3, while the purely even-parity interaction 5 is much more attractive than interaction 4 due to the strong local part of the interaction. In the Supplemental Material we also present an extension of our analysis to two spatial dimensions and find results which are similar to the one-dimensional results presented here [23].

Our conclusions corroborate the findings in Ref. [3] and suggest that the phenomenon of local dominance in the effective forces between quantum bound states is a universal feature appearing in other quantum systems, regardless of system details and dimensionality. Indeed, one can understanding the strength of van der Waals, ionic, covalent, metallic, and hydrogen bonding as being enhanced by the locality of the Coulomb interaction. Our results should also be useful in understanding the properties of composite bosons in designer quantum systems such as optical lattices.

There is much work left to do in understanding the nature of effective forces between quantum bound states. Many other systems must be studied with the same depth as we have pursued here. However, this simple study of dimers in one spatial dimension has already elucidated many important facets of the general phenomenon. We hope that these insights will lead to a deeper understanding of the connection between nuclear forces and nuclear structure. At a more practical level, we are already using some of these findings to develop new lattice chiral interactions with improved order-by-order convergence in *ab initio* nuclear structure calculations of medium mass nuclei.

We are grateful for discussions with Lucas Platter and for the hospitality of the Kavli Institute for Theoretical Physics at University of California Santa Barbara for hosting E. E., H. K., and D. L. We also acknowledge the partial financial support provided by the Deutsche Forschungsgemeinschaft (SFB/TR 110, "Symmetries and the Emergence of Structure in QCD"), the Bundesministerium für Bildung und Forschung (Verbundprojekt 05P2015—NUSTAR R&D), and the U.S. Department of Energy (Grant No. DE-FG02-03ER41260).

[1] F. London, Z. Phys. **63**, 245 (1930).
[2] E. Ruiz Arriola, arXiv:0709.4134.
[3] S. Elhatisari *et al.*, Phys. Rev. Lett. **117**, 132501 (2016).
[4] P. Maris, J. P. Vary, A. Calci, J. Langhammer, S. Binder, and R. Roth, Phys. Rev. C **90**, 014314 (2014).
[5] T. Duguet, V. Somà, S. Lecluse, C. Barbieri, and P. Navrátil, Phys. Rev. C **95**, 034319 (2017).
[6] S. R. Stroberg, A. Calci, H. Hergert, J. D. Holt, S. K. Bogner, R. Roth, and A. Schwenk, Phys. Rev. Lett. **118**, 032502 (2017).
[7] R. F. Garcia Ruiz *et al.*, Nat. Phys. **12**, 594 (2016).
[8] G. Hagen, G. R. Jansen, and T. Papenbrock, Phys. Rev. Lett. **117**, 172501 (2016).
[9] T. Dytrych, P. Maris, K. D. Launey, J. P. Draayer, J. P. Vary, D. Langr, E. Saule, M. A. Caprio, U. Catalyurek, and M. Sosonkina, Comput. Phys. Commun. **207**, 202 (2016).
[10] E. Epelbaum, H. W. Hammer, and U.-G. Meissner, Rev. Mod. Phys. **81**, 1773 (2009).
[11] M. Combescot and O. Betbeder-Matibet, Eur. Phys. J. B **48**, 469 (2005).
[12] M. Combescot, O. Betbeder-Matibet, and R. Combescot, Phys. Rev. B **75**, 174305 (2007).
[13] M. Combescot, O. Betbeder-Matibet, and F. Dubin, Phys. Rep. **463**, 215 (2008).
[14] W. V. Pogosov, M. Combescot, and M. Crouzeix, Phys. Rev. B **81**, 174514 (2010).
[15] L. Pilozzi, M. Combescot, O. Betbeder-Matibet, and A. D'Andrea, Phys. Rev. B **82**, 075327 (2010).
[16] E. Epelbaum, H. Krebs, T. A. Lähde, D. Lee, U.-G. Meißner, and G. Rupak, Phys. Rev. Lett. **112**, 102501 (2014).
[17] T. A. Lähde, E. Epelbaum, H. Krebs, D. Lee, U.-G. Meißner, and G. Rupak, Phys. Lett. B **732**, 110 (2014).
[18] T. A. Lähde, T. Luu, D. Lee, U.-G. Meißner, E. Epelbaum, H. Krebs, and G. Rupak, Eur. Phys. J. A **51**, 92 (2015).
[19] S. Elhatisari, D. Lee, G. Rupak, E. Epelbaum, H. Krebs, T. A. Lähde, T. Luu, and U.-G. Meißner, Nature (London) **528**, 111 (2015).
[20] D. S. Petrov, C. Salomon, and G. V. Shlyapnikov, Phys. Rev. Lett. **93**, 090404 (2004).
[21] D. S. Petrov, C. Salomon, and G. V. Shlyapnikov, Phys. Rev. A **71**, 012708 (2005).
[22] S. Elhatisari, K. Katterjohn, D. Lee, U.-G. Meißner, and G. Rupak, Phys. Lett. B **768**, 337 (2017).
[23] See Supplemental Material at http://link.aps.org/supplemental/10.1103/PhysRevLett.118.232502 for the extension to two spatial dimensions.